J Ther Eng, Vol. 11, No. 5, pp. 1276−1292, September, 2025

Journal of Thermal Engineering
Web page info: https://jten.yildiz.edu.tr
DOI: 10.14744/thermal.0000996

Research Article

Harnessing response surface methodology for diesel engine optimization using titanium dioxide-enhanced rice bran biodiesel to improve emissions and efficiency

Manoj Kumar GUPTA[1,*], Ashok Kumar SRIVASTAVA[2]

[1]*Research Scholar, Maharshi University of Information Technology, Lucknow, 226001, India*
[2]*Department of Mechanical Engineering, Maharshi University of Information Technology, Lucknow, 226001, India*

ARTICLE INFO

Article history
Received: 26 February 2025
Revised: 29 May 2025
Accepted: 31 May 2025

Keywords:
CI Engine; Optimization; Response Surface Methodology; Rice Bran Biodiesel; Titanium Dioxide Nanoparticles

ABSTRACT

The present work is associated with synergistic optimization and the effect of three operational variables, namely Load on the engine, rice bran biodiesel Blend, and TiO_2 Nanoparticle for emission attenuation of HC, CO_2, NOx, O_2, and CO, along with BTE amelioration of diesel engine sustainability. Under the category of Empirical Research work, Central Composite Design-based Response Surface Modeling and analysis of variance were done to find out the best suitable mathematical relationship with the most and least significant operational variable for all responses at a 95% level of confidence and 5% significance factor. Experimental data were obtained using a diesel engine test rig with biodiesel blends up to 30% and TiO_2 nanoparticles up to 200 ppm, under low, medium, and high load conditions. The responses were optimized using MINITAB with contour and surface plots.

The optimum combination of three operation parameters reported as 2.64094 kW engine Load, 30 ppm rice bran Biodiesel, and 141.742 ppm TiO_2 nanoparticles. Additionally, the optimal combination included CO 0.050% of the total sample, CO_2 3.30% of the total sample, HC 13.29 ppm, NO_X 385.78 ppm, and BTE 32.50%, resulting in a desirability effect of 73.74%; Improves BTE by 31.4% compared to pure diesel at low load and 22.9% at high load. A confirmation test run validates the result with a forecast error of less than 4%, with remarkable emissions reduction and performance gain of regular diesel engines without major changes, making it an eco-friendly option for the future.

Cite this article as: Gupta MK, Srivastava AK. Harnessing response surface methodology for diesel engine optimization using titanium dioxide-enhanced rice bran biodiesel to improve emissions and efficiency. J Ther Eng 2025;11(5):1276−1292.

INTRODUCTION

Diesel combustion in CI engines emits gases such as CO, CO_2, HC, NOx, and SOx, all of which contribute significantly to atmospheric pollution. These emissions are linked to environmental issues, including global warming, ozone depletion, acid rain, and reduced visibility. Human

***Corresponding author.**
*E-mail address: mail2manojgupta@gmail.com

This paper was recommended for publication in revised form by Editor-in-Chief Ahmet Selim Dalkılıç

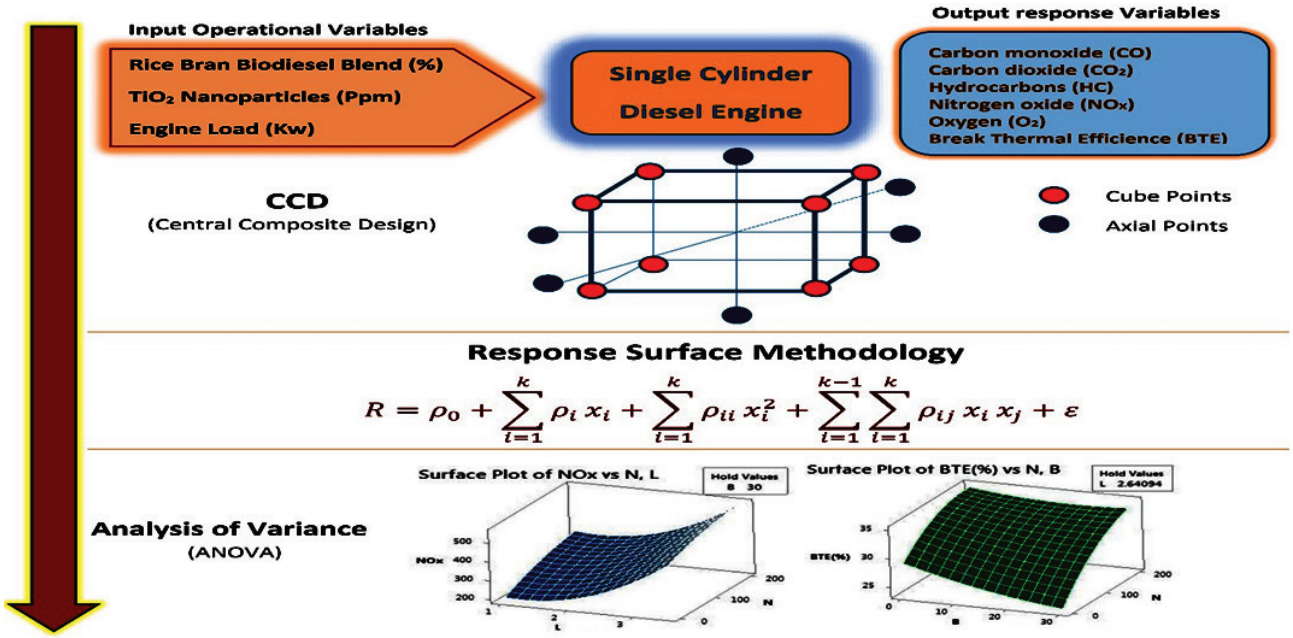

Figure 1. Graphical presentation of work.

exposure to these pollutants is associated with non-cancerous and cancerous health risks, such as respiratory issues, immune system damage, reproductive and neurological disorders, and cardiovascular diseases [1, 2, 3, 4].

As of 2021, the transportation sector accounts for 19% of global annual energy consumption. Projections by the International Energy Agency and Mobility 30 predict a 53% rise in global energy demand by 2030. According to the International Energy Outlook 2017, the energy share of on-road transportation stood at 13%, with on-road freight and passenger transport consuming 25.3 quadrillion British thermal units [5, 6, 7].

From now until 2030, oil use in road transport will increase by roughly 6 million barrels per day, with a particularly sharp increase in 2021, and it will climb by close to 8 million barrels per day in aviation, shipping, along petrochemicals [5]. Transport is a major source of pollution and climate change in the environment. Transport emissions, particularly from automobiles, contribute significantly to the levels of carbon dioxide in the atmosphere. With a range of 22 percent, transportation is the second-largest source of worldwide CO_2 emissions [8].

As a result of climate change, global warming is 0.8 ^{0}C above the level of pre-industrial, leading to a rise of sea level around 3.2 cm per decade. A rise of sea level of 0.5 to 1 meter is estimated before the 2060s by an increase of 4 ^{0}C global temperature. Although the greenhouse effect plays an impactful factor in global warming, naturally, though emission of transportation means has a major contribution. By 2100, the IPCC predicts a rise in global temperature of 1.1 to 6.4 degrees Celsius and a rise in global sea level of 7 to 23 inches, according to the Fourth Assessment Report. Global greenhouse emissions must be cut by 50–85 percent below 2000 levels by 2050, as per the IPCC, to keep warming to 2–2.4 degrees Celsius. To meet this goal, greenhouse emissions from all sectors must be decreased in a multi-generational effort [9, 10].

Therefore, several researchers are putting their effort into overcoming this problem by using alternative fuel to existing diesel engines without measuring the modification of the engine design. Biodiesel is one of the best choices of researchers as an alternative fuel due to its renewability, biodegradability, sulfur-free, non-toxic, and can greatly lower exhaust emissions [11,12].

In 2016, Vijayakumar Chandrasekaran et al. found that adding 50 ppm CuO nanoparticles to a 20% mahua biodiesel blend improved BTE by 2.19% and reduced HC, CO, and smoke emissions. However, NOx increased by 3.2%. The blend was considered a viable alternative for CI engines [13]. Mr. S. Padmanaba Sunder and his team found that using 200 ppm TiO_2 with plastic oil improved BTE by 2.64% and reduced HC by 18%. Additionally, 150 ppm TiO_2 decreased smoke opacity by up to 38% [14].

Samson K. Fasogbon in 2023 concluded that B20 biodiesel with 10 g/L Al_2O_3 nano-additive offers optimal CI engine performance and emissions [15]. Dhananjay Khankal in 2024 found that B10 mango kernel biodiesel improves BTE and BSFC over diesel. However, it shows higher CO_2 and NOx emissions at low injection pressure. At 25% load and high injection pressure, CO_2 and NOx emissions decrease by 12.5% and 13.23%, respectively, compared to diesel [16].

K. Yamini in 2024 found that isobutanol-based biodiesel) With 10% diethyl ether significantly reduced at full

load compared to diesel: HC by 24.39%, CO by 4.6%, NOx by 9.33%, and smoke opacity by 8.84% [17].

Researchers reported that biodiesel is comparable to conventional diesel with minimal impact on performance and emissions reductions. Additionally, it may be blended with conventional diesel or utilized as biodiesel oil in diesel engines. The use of biodiesel as an environmentally friendly fuel is growing in popularity [18, 19].

The literature review helps to find the answer: why my research work is important. It explains the problems with diesel engine pollution and the need for cleaner fuels. It also shows that biodiesel and nanoparticles can help, but most past studies looked at them separately. My review finds a gap very few studies have tested the combined effect of engine load, biodiesel, and nanoparticles or tried to find the best combination for optimization of the nanoparticle dose rate, which has yet to be done. The novelty of this work lies in the synergistic effect of three main operational variable engine load, rice bran biodiesel blend, and TiO_2 nanoparticles, to improve diesel engine performance. Unlike many studies that examine these variables independently, this study combines them using central composite design-based response surface methodology and ANOVA to develop meaningful models for emissions and engine performance. The use of rice bran biodiesel together with TiO_2 nanoparticles is an innovative approach to reduce engine emissions with a gain in performance without requiring any major modifications in the diesel engine making it a promising and environmentally friendly alternative for future diesel fuels.

Biodiesel Blends

Transesterification converts triglycerides to esters, which is how biodiesel is made from vegetable oils or animal fats. It possesses qualities that are similar to those of fossil diesel. Bio-diesel and environmentally beneficial diesel fuel alternatives for diesel engines [2, 20] . When compared to diesel fuel, biodiesel has a higher viscosity and density, as well as a higher cetane number, pour point, and flash point. Biodiesel is a full-oxygen fuel with a 10–15 percent oxygen content by weight and no sulfur [11, 21]. When compared to petro-diesel, using biodiesel in engines reduces CO, HC, and particulate matter emissions dramatically [22]. When burned as a fuel, biodiesel is appealing because it is biodegradable, sulfur-free, non-toxic, and can greatly lower exhaust emissions and overall life cycle CO_2 emissions from the engine, depending upon biodiesel blend as per ASTM standard [23, 24].

The emissions reduction advantage is roughly proportional to the blend level; for example, B20 has a 20% pollution reduction advantage over B100 [25, 26]. The load on the engine also has an impact on emission reduction. Researchers found that at full load, the mean BTE of Biodiesel blends was around 7 to 10 percent lower than that of pure diesel, but at lower loads, this variance was as high as 17 percent, which might be ascribed to Biodiesel blends much poorer efficiency, particularly at lower loads [11, 27, 28].

Nano Additives in Biodiesel Blend

Nano additives are nanoparticles that can improve the quality of biodiesel so that it can compete with diesel. The surface area of nanoparticles, where the heterogeneous reaction takes place, is much larger than that of bulk particles [29]. It increases the number of reaction sites available for the reaction to take place. The atoms on the surface are more unstable and reactive. This instability stems from their lattice location, which forces them to unbind their neighboring atoms or molecules [30, 31]. The instability and reactivity rise as the surface/bulk particles ratio increases. As a result, nanoparticles have a large surface-to-volume ratio [32, 33].

The use of nano-additives in biodiesel has substantial benefits, including increased lubricity, energy content, stability, and oxidation resistance [34]. These nanoparticles help to increase power output and reduce fuel consumption. Moreover, nano-additives improve heat transfer, catalytic activity, and fuel atomization, resulting in fewer NOx, CO, and hydrocarbon emissions. [35] These combined effects lead to improved fuel characteristics, better engine performance, lower emissions, and more efficient combustion procedures [36]. The small size of nano additives allows them to easily mix with biodiesel [13]. Furthermore, the addition of nanoadditives to some previously reported studies improved stability and other tribological features dramatically. This unique feature of Nano additives also aids in the elimination of wear/tear and choking concerns in CI engine parts [34, 36, 37].

Besides that, Qaisar Manzoor et al. (2024) reported that inhaled TiO_2 nanoparticles can accumulate in vital organs and are linked to oxidative stress, inflammation, and genotoxic effects, posing long-term health threats [38]. Jain et al. (2024) found that using TiO_2 nano-additives in diesel combustion increases fine and ultrafine particle emissions, which can penetrate deep into the lungs and pose serious respiratory health risks [39].

DESIGN OF EXPERIMENT

Depending upon operational conditions, examine how changes in variables (operational conditions) affect a desired response, along with choosing the right operational conditions to meet the requirements. [1, 40]

In this study, we are considering three continuous variables, denoted as L, B, and N. To obtain a design matrix by central composite design, the total number of experiments run is obtained by using a two-level full factorial equation

$$E = 2^n + 2n + n_0 \quad (1)$$

$E = 2^3 + (2*3) + 0$

$E = 14$

Where E = the total number of experiments

n = Number of Operational Variables
n0 = Center points in axial

Design Summary

Factors:	3	Replicates:	1
Base runs:	14	Total runs:	14
Base blocks:	1	Total blocks:	1

Two-level factorial: Full factorial

Point Types

Cube points:	8	Center points in cube:	0
Axial points:	6	Center points in axial:	0

Design Table (Randomized)

A single-cylinder, four-stroke diesel engine coupled with an eddy current-type dynamometer is taken into account to perform all experiments [41]. For online performance assessment, the LabVIEW-based Engine Performance Analysis software package is also present in the setup.

The maximum load-carrying capacity of the engine is 5 kW at a maximum rpm of 1500. It's an Indian make engine, made by Bharat DX, a very renowned name in the field of diesel engines. The engine has a stroke of 110 mm, a bore diameter of 87.5 mm, a cylinder volume of 661 cc, and a compression ratio (CR) of 17.5. It is fitted on a base frame having only one balance wheel and all other provisions for cooling water and temperature measurements.

Table 1. Experiment Run-Order Matrix with Formulations

Std Order	Run Order	Pt Type	Blocks	L Load (KW)	B Bio-Diesel Blend (%)	N Nano Particles (ppm)	Formulates
01	**02**	**03**	**04**	**05**	**06**	**07**	**08**
5	1	1	1	1.0	0	200	B0N200
8	2	1	1	3.5	30	200	B30N200
13	3	-1	1	2.0	15	0	B15N0
9	4	-1	1	1.0	15	100	B15N100
7	5	1	1	1.0	30	200	B30N200
12	6	-1	1	2.0	30	100	B30N100
3	7	1	1	1.0	30	0	B30N0
2	8	1	1	3.5	0	0	B0N0
6	9	1	1	3.5	0	200	B0N200
14	10	-1	1	2.0	15	200	B15N200
1	11	1	1	1.0	0	0	B0N0
11	12	-1	1	2.0	0	100	B0N100
10	13	-1	1	3.5	15	100	B15N100
4	14	1	1	3.5	30	0	B30N0

Table 1 presents a total of 14 experimental runs. Each run corresponds to a specific combination of three operational variables. The engine load varies from a minimum of 1.00 kW to a maximum of 3.50 kW, while the biodiesel blend ranges from 0% to 30%. The concentration of nanoparticles is adjusted between 0 ppm and 200 ppm. For each experimental run order, all six responses were recorded. To minimize errors in experimental data principle of replication is taken into account.

EXPERIMENTAL SETUP AND WORK

There are three parts to the work.

- Setting up the test rig
- Preparation of fuel as per the requirement of the experiment
- Collecting data by performing all experiments

Bharat DX makes an eddy current-based dynamometer of 5 KVA capacity with 1500 rpm at 50Hz. The dynamometer is directly connected to the engine shaft. It is also fixed in the same frame. It is air-cooled, so easy to operate and maintain. The output of the dynamometer is directly connected to the Rheostat.

A rheostat of capacity 3.5 kW is used to create a load on the engine. There are a total of seven loads, each of 0.5 kW, arranged. Each load has an individual ON-OFF switch, and a main Power Switch is used to put the load on the engine. By operating individual ON-OFF switches load can be applied in additional order.

To measure exhaust gas AIRVISOR model number AVG-500 was used. It is interconnected to the computer system. The probe of the gas analyzer is inserted into the exhaust line of the engine. The airvisor itself has a small display

unit to display all parameters associated with exhaust gas measurement.

The blending of biodiesel and nanoparticles with pure diesel fuel has some issues, like biodiesel has high viscosity and density, leading to poor fuel atomization and combustion [11, 22]. It also has poor cold flow properties, causing starting problems in low temperatures [22], and oxidation instability, which affects long-term storage [34]. Other issues include phase separation, injector clogging, and material compatibility with rubber parts [27, 28]. To reduce these problems, transesterification is used. This chemical process converts raw oils into biodiesel with lower viscosity and better fuel properties, improving blending and engine compatibility.

For nanoparticles, the main issues are agglomeration, poor dispersion, and settling down during storage, which reduces effectiveness and may block injectors [36]. To address this, ultrasonication is used. High-frequency sound waves break up clumps and evenly disperse nanoparticles in the fuel. This method ensures better suspension, stable blending, and improved combustion. Together, transesterification and ultrasonication provide effective solutions for improving the stability, performance, and safety of biodiesel–nanoparticle blends in diesel engines.

Uncertainties Associated and Minimization

To minimize errors and variability in experimental measurements, the following steps were taken:

1. Fuel blending inconsistencies: Standardize blending procedures, implement quality control, and verify fuel composition through comparative before-use analysis.
2. Ambient condition variations: Conduct experiments in controlled environments, monitor conditions, and calibrate instruments for environmental factors.
3. Instrument calibration limitations: using regularly calibrated instruments, high-precision equipment, and validating results against reference methods.

To reduce uncertainties (errors) in experimental data measurement; the principle of replication is used to find the best experimental result. At its core, replication means repeating an experiment or measurement under the same parameters till the same response of the last two consecutive runs to assess variability, reduce random error, and increase confidence in the conclusions drawn. In the analysis phase, replication provides degrees of freedom for the estimation of the error term. That's why in ANOVA, the error term is calculated from the deviations within each replicated group with a 95% level of confidence and 5% significance factor. More replications mean a more accurate and stable estimate of the error variance.

In this work, the Central Composite Design under RSM also helps to reduce uncertainty by minimizing the number of experiments while still giving a statistically strong model.

Blended Fuel with Nanoparticle Formulation

Firstly, as per the ASTM D6751 standard, the rice bran biodiesel, supplied by a reputable Indian supplier, was blended with pure diesel sourced from a well-known Indian company's filling station, according to the design matrix [23]. TiO_2 in powder form, procured from Adnano, Karnataka, India, was then added to the rice bran biodiesel-diesel mixture, following the design matrix, to produce a stable nanofluid solution [42, 43]. To prevent nanoparticle agglomeration, the TiO_2-blended biodiesel underwent ultrasonication using a bath-type ultrasonicator operating at a frequency of 40 kHz and a power of 80W for three hours at a temperature of 30-40°C, resulting in a clear, stable solution [15]. Following this, transesterification was carried out, and a high-shear magnetic mixer was used to

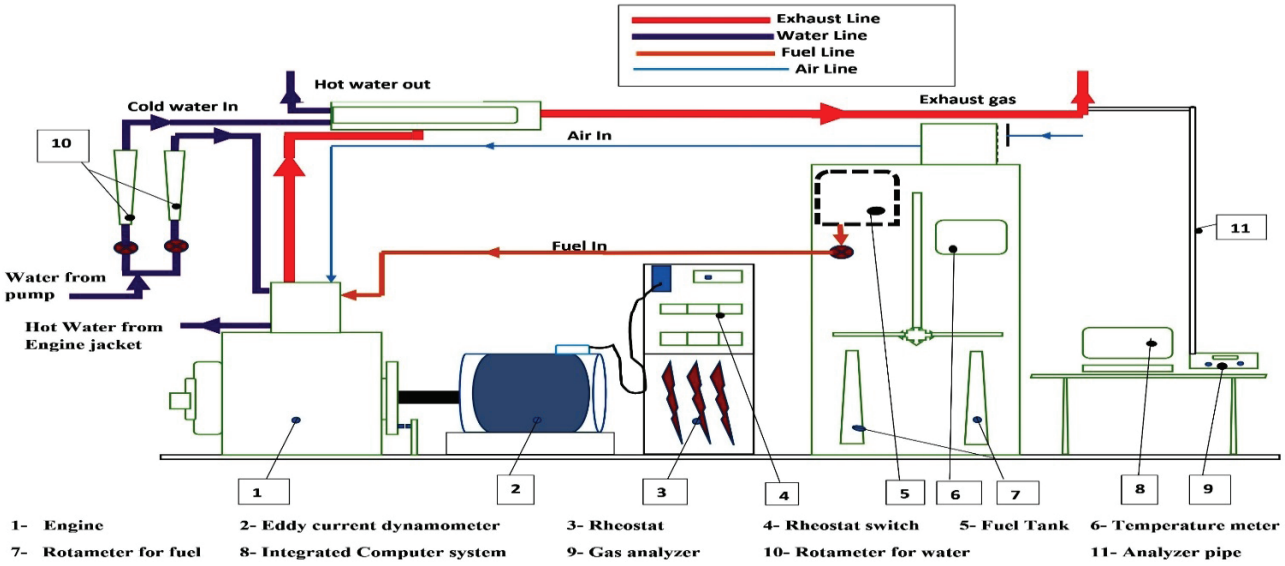

Figure 2. Schematic line diagram of test rig.

ensure thorough mixing for two hours at 40°C. This process applied mechanical force to evenly disperse the nanoparticles in the biodiesel, producing a homogeneous, stable solution free from sedimentation [44]. The formulation of fuel is given in Table 01 in column no. 08.

Observation Table for Experiment Run Order

Table 2 shows the different parameter values obtained during the operation of the diesel engine test rig. Column no. 01 shows the experiment run order no as per DOE. Column no. 02 shows the fuel used for the experiment. Column 03 shows the loan on the engine in Kw. Column no. 04 shows the time in minutes and seconds to consume 20ml of fuel. Columns no-05 to 09 show the value of different response variables.

Calculation of Performance Parameters

Total fuel consumption (TFC)

Total fuel consumption denotes the fuel consumed per unit of time. The unit of TFC is Kg/Sec.

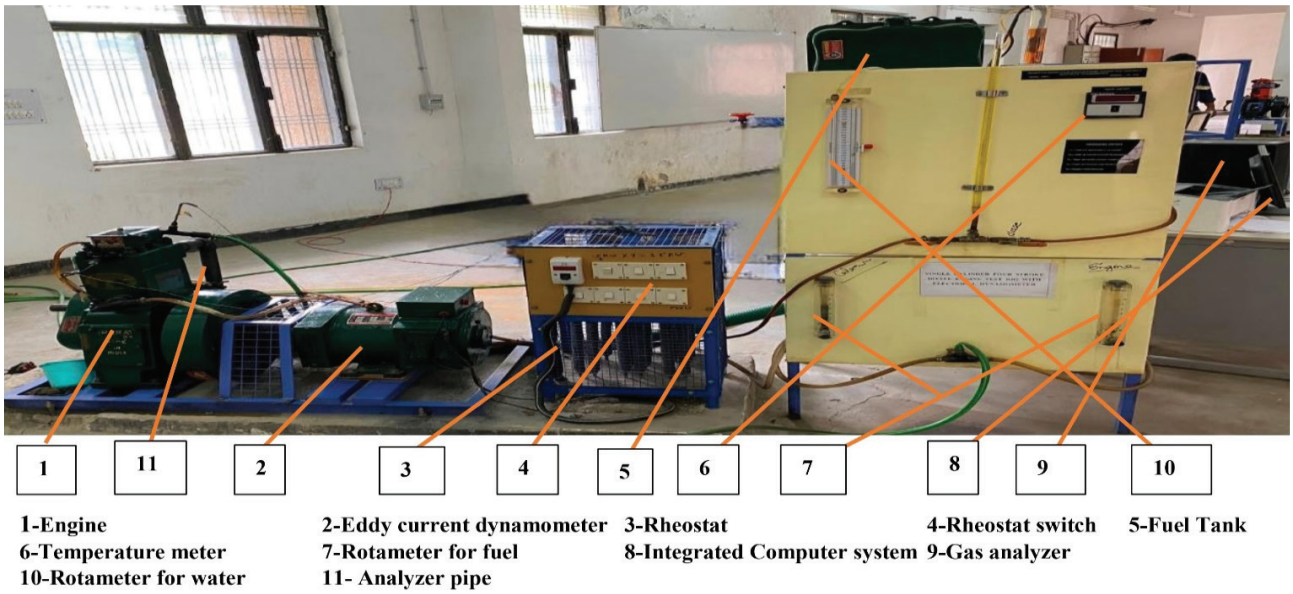

Figure 3. Actual test rig.

Table 2. Diesel Engine Test Rig Observation Data

Run Order	FUEL	Load	20ml Fuel consumption time (Sec)	HC	CO_2	NOx	O_2	CO
01	02	03	04	05	06	07	08	09
1	B0N200	1.0	225.3	29	2.60	305	18.53	0.08
2	B30N200	3.5	74.3	14	4.40	552	15.87	0.06
3	B15N0	2.0	86.9	25	3.40	300	14.90	0.05
4	B15N100	1.0	180.9	30	2.50	280	18.23	0.07
5	B30N200	1.0	200.4	26	2.40	330	18.34	0.07
6	B30N100	2.0	107	16	3.20	303	16.40	0.06
7	B30N0	1.0	113.2	30	2.50	233	17.75	0.07
8	B0N0	3.5	54.4	9	4.50	556	14.35	0.04
9	B0N200	3.5	68.8	9	4.20	578	17.80	0.06
10	B15N200	2.0	124.7	25	3.20	350	16.80	0.06
11	B0N0	1.0	178.0	27	2.70	257	16.45	0.06
12	B0N100	2.0	124.2	12	3.30	332	16.20	0.06
13	B15N100	3.5	64.5	14	4.65	520	15.65	0.05
14	B30N0	3.5	47.3	19	4.70	501	13.69	0.06

$$TFC = \frac{Fuel\ consumed}{Time} \times \frac{Specific\ Gravity}{1000} \quad (2)$$

Where
Fuel consumed in ml
Time in Seconds

Brake-specific fuel consumption (BSFC)

Brake-specific fuel consumption is the total fuel consumption per unit brake bower. Here, the unit of BSFC is Kg/kW Hr.

$$BSFC = \frac{TFC}{BP} \times 3600 \quad (3)$$

Where
TFC is total fuel consumption in Kg/Sec
BP is load in kW

1.1.1 Brake thermal efficiency (BTE)

It is calculated by the following equation

$$BTE = \frac{BP}{TFC \times CV} \times 100 \quad (4)$$

Where
BP is load in kW
TFC is total fuel consumption in Kg/Sec
CV is the Calorific value of fuel in KJ/Kg

RESULTS AND ANALYSIS

As per the design of the experiment, all 14 sets of operation variable tests were performed, and the 06 response variables were recorded along with the engine performance parameters. All values are given below in Table 3.

Table 6 shows that the regression models for all response variables (HC, CO_2, NO_X, O_2, CO, and BTE) are highly accurate, with R^2 values above 99% in most cases. The low standard error (S) indicates a good fit, and the high adjusted and predicted R^2 values confirm strong model performance and reliability in predictions. Overall, all models are robust and well-suited for analysis and prediction.

The confidence level of analysis is taken at 95%, so the significance factor (α) is 5%. If the significance factor of any response variable for any operational variable is more than 5% ($P > 0.05$), then it means the null hypothesis is satisfied and indicates no dependence on the operational variable. If it is less than 5% ($P \leq 0.05$), then it means the null hypothesis is rejected and the alternate hypothesis is accepted, suggesting a significant impact of the operational variable [40].

Tables 4 and 5 show that all three operational variables (L, B, and N) significantly affect all six responses ($P \leq 0.05$). For HC and CO_2, the load (L) is the most significant factor due to its lowest p-value and highest F-test value, while biodiesel (B) is the least significant. For NOx, L is again the most significant, while nanoparticle (N) is the least. In the case of O_2, L is most significant, followed by N, while B remains the least significant.

Table 3. Result table for each run-order

Run Order NO	FUEL	Load	20ml Fuel consumption time (Sec)	HC (ppm)	CO_2 (% of total Sample)	NOx (ppm)	O_2 (% of the total sample)	CO (% of the total sample)	TFC (Kg/Hr)	BSFC (Kg/Kw Hr)	BTE (%)
01	02	03	04	05	06	07	08	09	10	11	12
1	B0N200	1.0	225.3	29	2.60	305	18.53	0.08	0.2690	0.2690	30.2
2	B30N200	3.5	74.3	14	4.40	552	15.87	0.06	0.8279	0.2365	33.5
3	B15N0	2.0	86.9	29	3.40	287	14.90	0.05	0.6899	0.3449	24.7
4	B15N100	1.0	180.9	30	3.40	305	18.23	0.07	0.3342	0.3342	24.5
5	B30N200	1.0	200.4	26	2.30	330	18.34	0.08	0.3071	0.3071	25.8
6	B30N100	2.0	107	16	2.80	303	16.40	0.05	0.5718	0.2859	28.4
7	B30N0	1.0	113.2	30	2.50	202	17.75	0.065	0.5327	0.5327	15.8
8	B0N0	3.5	54.4	14	4.90	556	14.35	0.06	1.0982	0.3137	26.2
9	B0N200	3.5	68.8	9	3.50	472	17.80	0.06	0.8801	0.2514	32.3
10	B15N200	2.0	124.7	25	2.80	305	16.80	0.055	0.4894	0.2447	32.8
11	B0N0	1.0	178.0	32	4.10	357	16.45	0.08	0.3355	0.3355	24.5
12	B0N100	2.0	124.2	16	3.30	340	16.20	0.06	0.4843	0.2421	33.9
13	B15N100	3.5	64.5	15	4.90	520	15.65	0.05	0.9367	0.2676	30.6
14	B30N0	3.5	47.3	19	4.40	458	13.69	0.05	1.2754	0.3644	23.1

Table 4. ANOVA table for CO_2, $NO_{X,}$ and O_2

Source	DF	HC				CO2				NOX			
		Adj SS	Adj MS	F-Value	P-Value	Adj SS	Adj MS	F-Value	P-Value	Adj SS	Adj MS	F-Value	P-Value
Model	9	776.604	86.289	1363.32	0.000	10.1657	1.12952	252.90	0.000	162380	18042	1914.62	0.000
Linear	3	625.551	208.517	3294.44	0.000	6.8949	2.29831	514.59	0.000	116375	38792	4116.52	0.000
L	1	577.600	577.600	**9125.72**	**0.000**	5.1840	5.18400	**1160.70**	**0.000**	112148	112148	**11901.01**	**0.000**
B	1	3.304	3.304	**52.21**	**0.002**	0.3546	0.35459	**79.39**	**0.001**	3214	3214	**341.03**	**0.000**
N	1	44.647	44.647	**705.39**	**0.000**	1.3563	1.35634	**303.69**	**0.000**	1013	1013	**107.51**	**0.000**
Square	3	131.582	43.861	692.97	0.000	1.1623	0.38744	86.75	0.000	16984	5661	600.76	0.000
L*L	1	10.571	10.571	167.02	0.000	1.0291	1.02907	230.41	0.000	14952	14952	1586.68	0.000
B*B	1	86.779	86.779	1371.05	0.000	0.2309	0.23087	51.69	0.002	178	178	18.87	0.012
N*N	1	63.087	63.087	996.73	0.000	0.1616	0.16163	36.19	0.004	711	711	75.49	0.001
2-Way Interaction	3	29.922	9.974	157.58	0.000	1.5879	0.52929	118.51	0.000	18107	6036	640.50	0.000
L*B	1	28.651	28.651	452.66	0.000	0.6675	0.66746	149.44	0.000	1556	1556	165.07	0.000
L*N	1	1.146	1.146	18.11	0.013	0.0092	0.00917	2.05	0.225	531	531	56.35	0.002
B*N	1	0.125	0.125	1.97	0.233	0.9112	0.91125	204.03	0.000	16021	16021	1700.07	0.000
Error	4	0.253	0.063			0.0179	0.00447			38	9		
Total	13	776.857				10.1836				162418			

Table 5. ANOVA table for O_2, CO, and BTE

Source	DF	O2				CO				BTE			
		Adj SS	Adj MS	F-Value	P-Value	Adj SS	Adj MS	F-Value	P-Value	Adj SS	Adj MS	F-Value	P-Value
Model	9	30.0541	3.3393	151.45	0.000	0.001676	0.000186	78.39	0.000	331.000	36.778	109.04	0.000
Linear	3	25.1588	8.3863	380.34	0.000	0.001111	0.000370	155.90	0.000	264.049	88.016	260.95	0.000
L	1	14.2564	14.2564	**646.56**	**0.000**	0.000903	0.000903	**379.84**	**0.000**	62.001	62.001	**183.82**	**0.000**
B	1	0.2151	0.2151	**9.75**	**0.035**	0.000120	0.000120	**50.64**	**0.002**	39.644	39.644	**117.54**	**0.000**
N	1	10.6873	10.6873	**484.69**	**0.000**	0.000088	0.000088	**37.21**	**0.004**	162.404	162.404	**481.50**	**0.000**
Square	3	2.3353	0.7784	35.30	0.002	0.000608	0.000203	85.33	0.000	48.533	16.178	47.96	0.001
L*L	1	2.1198	2.1198	96.14	0.001	0.000327	0.000327	137.75	0.000	29.190	29.190	86.54	0.001
B*B	1	0.0071	0.0071	0.32	0.600	0.000054	0.000054	22.76	0.009	1.000	1.000	2.97	0.160
N*N	1	0.3865	0.3865	17.53	0.014	0.000012	0.000012	4.96	0.090	7.647	7.647	22.67	0.009
2-Way Interaction	3	3.8418	1.2806	58.08	0.001	0.000085	0.000028	11.91	0.018	25.666	8.555	25.36	0.005
L*B	1	1.7824	1.7824	80.84	0.001	0.000004	0.000004	1.64	0.270	16.343	16.343	48.45	0.002
L*N	1	1.1072	1.1072	50.21	0.002	0.000003	0.000003	1.20	0.334	0.078	0.078	0.23	0.656
B*N	1	0.9522	0.9522	43.18	0.003	0.000078	0.000078	32.88	0.005	9.245	9.245	27.41	0.006
Error	4	0.0882	0.0220			0.000010	0.000002			1.349	0.337		
Total	13	30.1423				0.001686				332.349			

Table 6. ANOVA model assessment

Model	S	R-sq	R-sq(adj)	R-sq(pred)
HC	0.251582	99.97%	99.89%	99.43%
CO2	0.0668302	99.82%	99.43%	98.07%
NOX	3.06976	99.98%	99.92%	99.77%
O2	0.148491	99.71%	99.05%	96.79%
CO	0.0015414	99.44%	98.17%	91.56%
BTE	0.580766	99.59%	98.68%	95.95%

Table 7. Regression relation of variables

HC =	44.293 - 13.537L + 0.6122B - 0.11437N + 1.388L * L - 0.026389B * B + 0.000506N * N + 0.10053L * B - 0.003016L * N - 0.000083B*N
CO_2 =	5.281 - 1.630L - 0.02876B - 0.002544N + 0.4332L * L - 0.001361B * B - 0.000026N * N + 0.01534L * B + 0.000270L * N + 0.000225B*N
NOx =	459.14 - 154.86L - 6.980B + 0.1393N + 52.21L * L + 0.03778B * B - 0.001700N * N + 0.7407L * B - 0.06492L*N + 0.029833B * N
O_2 =	19.510 - 3.673L + 0.0625B + 0.01505N + 0.6217L * L + 0.000239B * B - 0.000040N * N - 0.02507L * B + 0.002964L * N - 0.000230B * N
CO =	0.11481 - 0.04244L - 0.001148B - 0.000035N + 0.007725L * L + 0.000021B * B + 0.00000N * N + 0.000037L * B - 0.000005L * N + 0.000002B * N
BTE =	15.64 + 11.16L - 0.4604B + 0.06307N - 2.307L * L + 0.00283B * B - 0.000176N * N + 0.0759L * B + 0.00079L * N + 0.000717B*N

For CO, L is the most significant operational variable, with B being the second most significant, and N the least. In BTE analysis, N is the most significant, followed by L, with B being the least. These trends are further supported by the sum of squares (SS) data for each operational variable.

The ANOVA model assessment is presented in Table 6, showing that values of R-sq, R-sq (adj), and R-sq (pred) are more than 90% for each response. All values of R^2 are very high, so it means the model is highly matched with the experimental data. The equations presented in Table 7 employ the least-squares method to derive second-order polynomial equations corresponding to each distinct engine response.

Response Optimization: BTE, CO, NOX, CO_2, HC

Response Optimizer Function of Minitab software with 95 % of the lower bound confidence level of all intervals is used to optimize the responses with the following inputs-

Parameters

The goal of minimization was set for four emissive responses: HC, CO_2, NOx, and CO; out of five emissive responses, except O_2. Since O_2 is not a harmful emissive, so does not need to be optimized. BTE is set for maximum. All responses have the same weightage and responses as given in Table 8.

Variable Ranges

The range of operation variables is set as per the given Table 9.

Table 8. Table of parameters of responses to rsm

Response	Goal	Lower	Target	Upper	Weight	Impor tance
BTE(%)	Maximum	15.8	33.90		1	1
CO	Minimum		0.05	0.08	1	1
NOx	Minimum		202.00	556.00	1	1
CO_2	Minimum		2.30	4.90	1	1
HC	Minimum		9.00	32.00	1	1

Table 9. Table of variable range for RSM

Variable	Values
L	(1, 3.5)
B	(0, 30)
N	(0, 200)

Solution

The optimization results show a fair balance between emissions (CO, NOx, CO_2, HC) and efficiency (BTE), with a desirability score of 0.737499. The Brake Thermal Efficiency is optimized to 32.51%, while emissions are minimized, indicating a reasonably effective balance between efficiency and emissions.

Figure 10 shows the nature and variations of each response concerning each operation variable for the optimized result, the solution obtained in Table No. 10.

Surface Plots of Optimized Responses

The set of figures (Figures 4 to 9) illustrates various surface plots of different emissions and parameters, each plotted against combinations of variables B & L, N & L, and N & B.

Starting with the HC plots, the first graph shows that B and L parameters are influencing in a coordinated way, leading to an interplay that can result in varying HC concentrations depending on their respective values. This

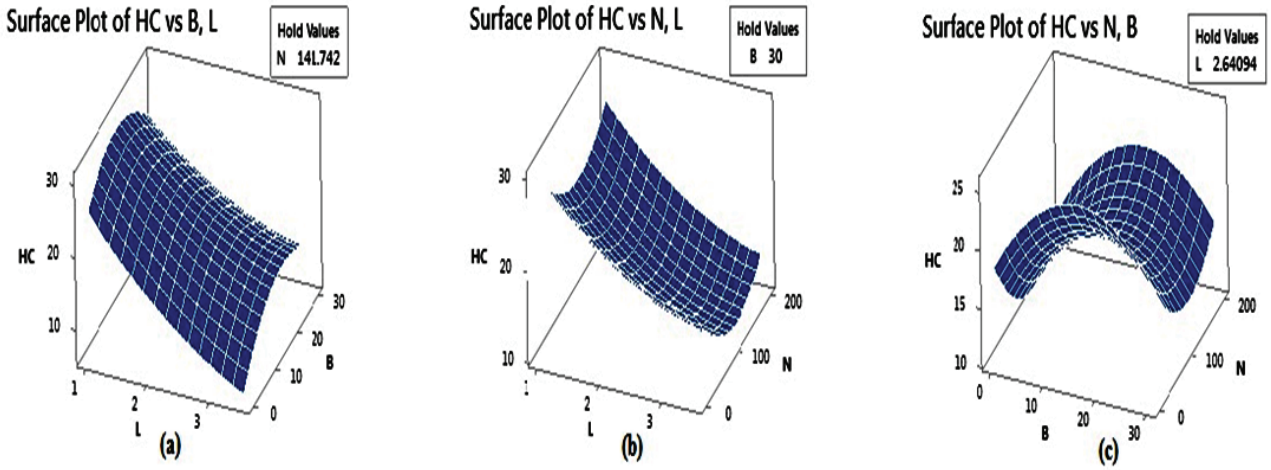

Figure 4. Surface Plot of HC with respect to (a) B&L, (b) N&L, (c) N&B.

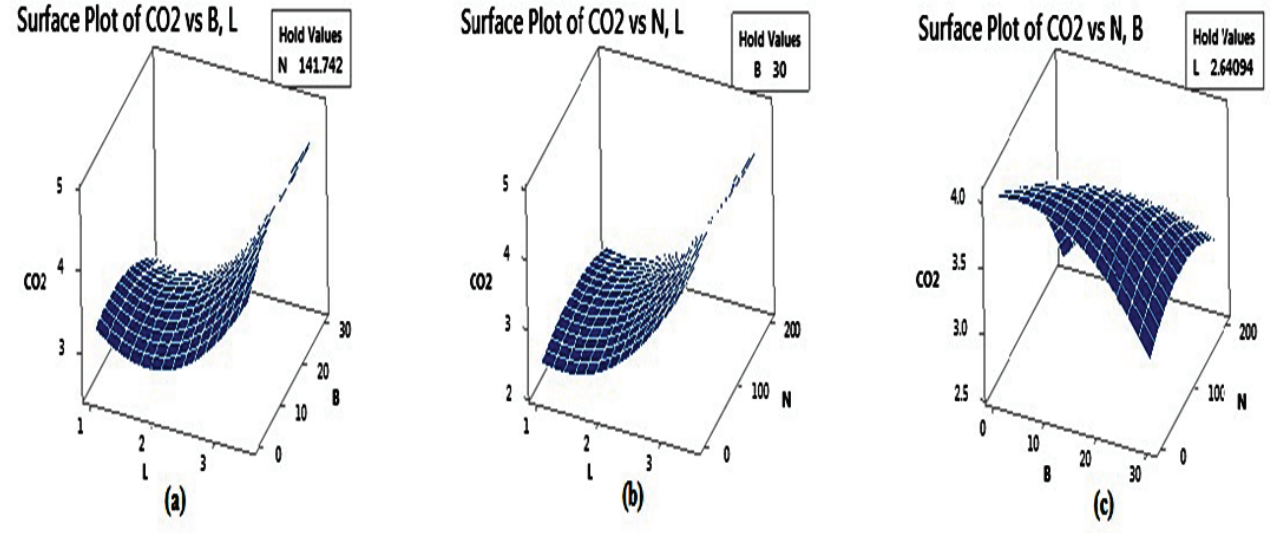

Figure 5. Surface Plot of CO_2 with respect to (a) B&L, (b) N&L, (c) N&B.

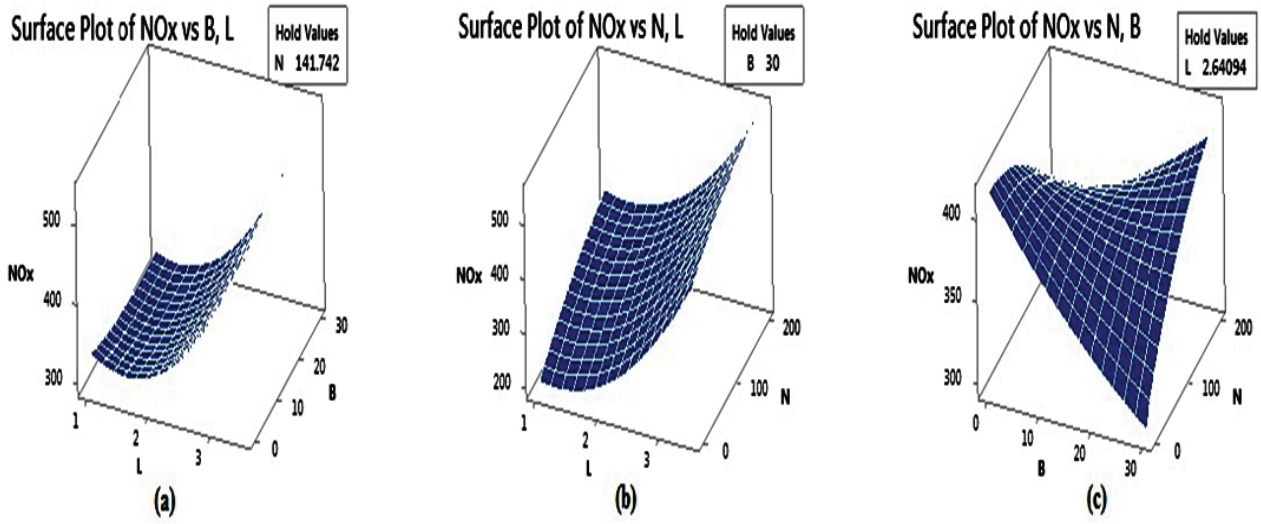

Figure 6. Surface Plot of NOX with respect to (a) B&L, (b) N&L, (c) N&B.

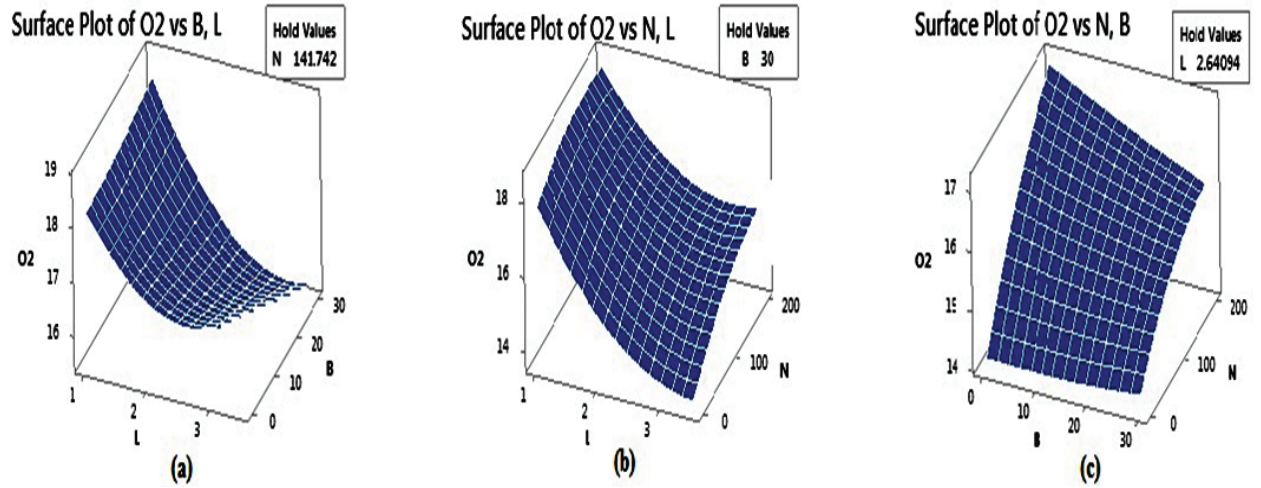

Figure 7. Surface Plot of O_2 with respect to (a) B&L, (b) N&L, (c) N&B.

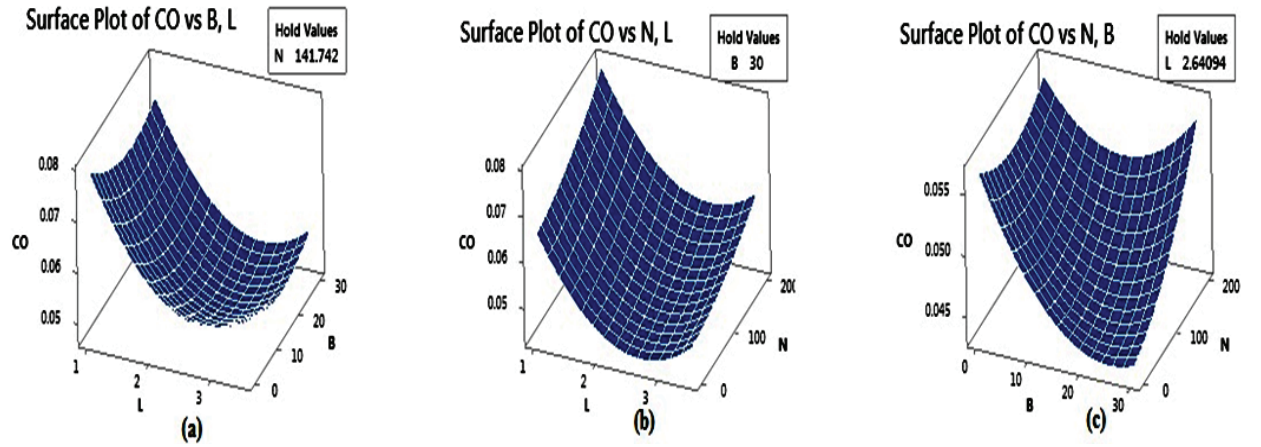

Figure 8. Surface Plot of CO with respect to (a) B&L, (b) N&L, (c) N&B.

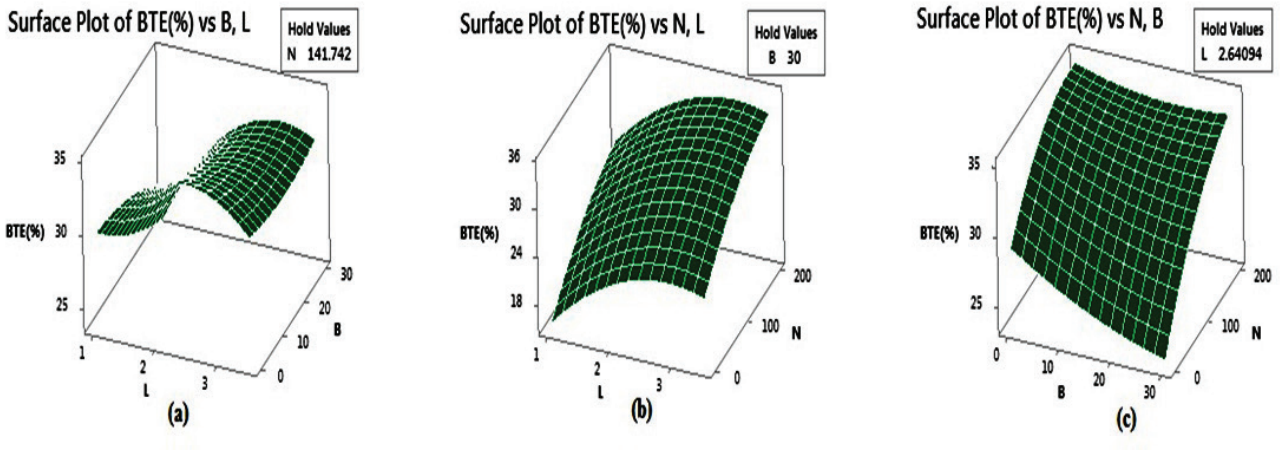

Figure 9. Surface Plot of BTE with respect to (a) B&L, (b) N&L, (c) N&B.

Table 10. Optimize solution by RSM

Variables	Solution
L	2.64094
B	30.00
N	141.742
BTE (%) Fit	32.5088
CO Fit	0.0504219
NOx Fit	385.780
CO_2 Fit	3.30655
HC Fit	13.2912
Composite Desirability	0.737499

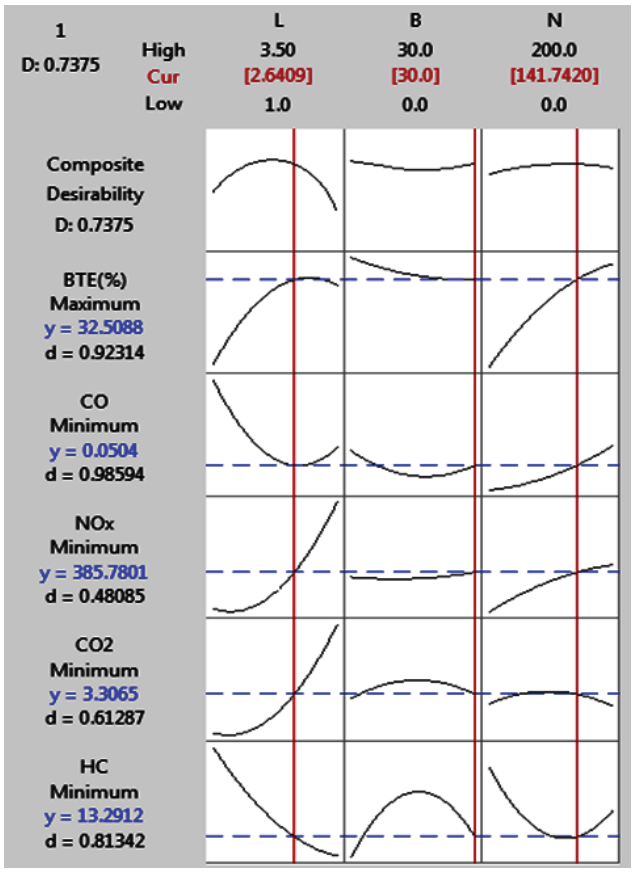

Figure 10. Optimization of responses.

suggests that biodiesel, possibly due to its cleaner combustion properties, leads to lower HC emissions, especially at higher loads. In the second plot of HC versus N and L, the non-linear behavior suggests a more complex relationship between these two, where increasing one or both has a significant and potentially non-additive impact on HC levels, with nanoparticles contributing to a further reduction in HC emissions as load increases. The third HC plot, which examines N and B, indicating strong nonlinear interactions, implies that when varied together, they have a pronounced effect on HC emissions, mostly magnifying or reducing emissions. This might be due to the way nanoparticles enhance combustion or act as catalysts.

The first plot of CO_2 shows a surface that gradually rises. This indicates that both variables, B and L, contribute to increasing CO_2 emissions, as would be expected in a combustion process where higher loads require more fuel. Biodiesel shows a modest effect on CO_2 levels, which might be due to the chemical composition of biodiesel itself. In the second CO_2 plot, the surface still exhibits a slight curvature, indicating that variables do interact, although the effect seems more gradual [30]. The third CO_2 plot shows more curvature than the first two, suggesting that N and B together have a more dynamic effect on CO_2 emissions.

The first NO_X plot shows a gentle slope, suggesting that as B and L increase, NO_X levels rise, but the surface

suggests that this increase is smoother compared to the HC and CO_2 cases. In the second NO_X plot, a stronger upward curve is observed, indicating that as either N or L increases, NO_X levels rise more sharply, particularly when both variables are at higher levels due to a non-linear relationship. The third NO_X plot reveals the most complex surface of the three, with the possibility of both variables either amplifying or mitigating each other's impact on the system.

The first plot of O_2 shows that oxygen levels decrease as both load and bio-diesel concentration increase. This suggests that higher loads and more biodiesel content in the blend result in a richer combustion process, which consumes more oxygen. In the second plot, as the load increases and the nanoparticle concentration rises, oxygen levels tend to decrease. This trend implies that the introduction of nanoparticles, along with an increased load, intensifies the combustion process, leading to more oxygen being consumed. The third plot of O_2 examination shows that Oxygen concentration decreases as both nanoparticle and bio-diesel content increase, again indicating more complete combustion with higher bio-diesel and nanoparticle concentrations [45].

The first plot of CO, which focuses on the relationship between B and load L, shows a slight increase in CO emissions as both variables increase. This suggests that under higher loads and with higher bio-diesel content, incomplete combustion becomes more likely, producing more CO. The second plot shows that as load increases, CO levels tend to decrease slightly, while increasing nanoparticle content results in higher CO emissions. The nanoparticles might enhance combustion efficiency [29]. The third plot of CO shows that CO emissions decrease as nanoparticle concentration rises, but at the same time, CO increases slightly as bio-diesel concentration increases. This behavior could be due to the complex interaction between bio-diesel properties and nanoparticle effects on the combustion process.

At the last the very first surface plots of BTE, the brake thermal efficiency tends to increase with moderate loads and bio-diesel concentrations, but starts to decline when either load or bio-diesel concentration becomes too high. This suggests that the combustion process is most efficient at moderate levels of load and bio-diesel, but higher loads and bio-diesel concentrations lead to inefficiencies, possibly due to incomplete combustion or higher exhaust losses. In the second plot, N and L affect BTE, with B held constant. Here, BTE generally increases as nanoparticle concentration rises, indicating that nanoparticles help improve the combustion process by enhancing the heat release and improving the overall efficiency [46]. However, higher loads seem to reduce efficiency after a certain point. The third plot, which explores the effect of nanoparticle concentration and bio-diesel content with a load constant, reveals that brake thermal efficiency increases with nanoparticle concentration, especially at higher bio-diesel levels. This suggests that the addition of nanoparticles into the bio-diesel blend helps to counteract some of the efficiency losses typically associated with using bio-diesel by improving combustion stability and heat transfer.

Validation

The optimization results obtained by RSM had a desirability of 0.737 for engine load 2.64 KW, rice bran bio-diesel blend 30 Ppm, and TiO_2 nanoparticle 141.74 Ppm. To fulfill the objective of the current work, the validation of these new findings is necessary, so a confirmation experiment is done by taking operational variables:

Table 11. Properties of conformation test fuel [47, 48, 49]

Fuel	Time in Sec (20ml consumption of fuel)	Specific gravity	Viscosity (mm^2/Sec)	Calorific value (KJ/Kg)	Load (Kw)	TFC (Kg/Hr)	BSFC (Kg/Kw Hr)
B30N150	98.5	0.852	4.58	44880	2.5	0.6227	0.24908

Table 12. Verification experiment test of responses

Responses	Predicted value	Experimental value	Error (%)
BTE	32.56	32.2	1.11
CO	0.051	0.05	2.0
O_2	15.71	15.25	3.01
NO_x	385.78	375	2.87
CO_2	3.30	3.2	3.12
HC	13.29	13	2.23

Load (L) = 2.5 Kw
Rice bran bio-diesel (B) = 30 Ppm
TiO_2 nanoparticle (N) = 150 Ppm

Here, the operational variable's value is taken to the nearest complete factors of optimized results due to the ease of setting up of experiment on the engine. Here, the principle of replication is used to find the best experimental result. The properties of the fuel are:-

In addition, projected values identified with the help of the model were utilized for validation, together with experimental values. The percentage of errors displayed in Table 12, demonstrates that the proposed models, which incorporate RSM for BTE, CO, NOx, CO_2, HC, and O2, are reasonably capable of predicting the impact of 2.5 Kw engine load, 30 Ppm rice bran biodiesel blend, and 150 Ppm TiO_2 nanoparticle on diesel engine combustion. Since the expected error is less than 4%, it is acceptable and should be approved.

These findings demonstrate the potential of rice bran biodiesel blended with TiO_2 nanoparticles as a clean, efficient fuel for CI engines. The optimized parameters reduce emissions and improve engine performance, making this approach suitable for practical applications. Future research can focus on scaling, exploring alternative nanoparticles, long-term engine impact, and integration with smart engine control systems to advance sustainable fuel technologies.

CONCLUSION

As per the objective, the present work is associated with synergistic optimization and the effect of three operational variables, namely Load on the engine, rice bran biodiesel Blend, and TiO_2 Nanoparticle for emission attenuation of HC, CO_2, NOx, O_2, and CO along with BTE amelioration of diesel engine sustainability. Because of the criticalness of these responses to estimate the suitability of fuel under the influence of operational variables. The main observations are given below:-

1. The utilization of transesterification and ultrasonic techniques to produce a blend of rice bran biodiesel and TiO_2 nanoparticles has resulted in a fuel that meets the specifications outlined in the ASTM biodiesel standard, making it a viable option for use in CI engines.
2. By utilizing Central Composite Design-based Response Surface Modeling, a Design of Experiments approach can potentially identify the optimal parameter settings necessary to achieve the desired level of performance. This can be accomplished through the use of the composite desirability method, which can provide a reasonably accurate estimation of the required parameter values.
3. The optimum combination of three operation parameters is determined and reported as 2.64094 kW engine Load, 30 ppm Rice bran Bio-Diesel blend, and 141.742 ppm TiO2 nanoparticles.
4. Additionally, the desired outcomes at the previously mentioned optimal combination included 0.050% of total sample CO, 3.30% of total sample CO_2, 13.29 ppm of HC, 385.78 ppm of NOx, and a BTE of 32.50%, resulting in a desirability effect of 73.74%.
5. The experimental data were used to validate the results, and the validation showed an error of 1.11% for BTE, 2.0% for CO, 3.01% for O_2, 2.87% for NOx, 3.12% for CO_2, and 2.23% for HC. These errors were within a range of below 4%.
6. Compared to earlier studies, the current work shows significant improvements. Vijayakumar et al. (2016) achieved only a 2.19% BTE increase and limited emission reductions using 20% mahua biodiesel with 50 ppm CuO. Padmanaba Sunder et al. (2021) reported a 2.64% BTE gain with 200 ppm TiO_2 in plastic oil. In contrast, our study using B30N150 at a 2.5 kW load outperforms pure diesel in both terms, of emissions and efficiency. It reduces HC by 59.4% at low load and 7.1% at high load. CO_2 emissions drop by 21.95% at low load and 34.7% at high load. CO is significantly reduced by 69.7% under low load and 16.7% under high load. Under low load, NOx increases by 5.0 percent. But under high load, it is reduced by 32.5 percent. The blend of 30% rice bran-biodiesel and 150 ppm TiO_2 nanoparticles improves BTE by 31.4% compared to pure diesel at low load and 22.9% at high load. The B30N150 improves combustion, which leads to remarkable BTE amelioration and emission attenuation.

This study provides valuable insights into the optimization of combustion parameters for rice bran biodiesel blends with TiO_2 nanoparticles. This means the fuel is cleaner and more efficient overall. Since it works well in regular diesel engines without major changes, it could help meet strict pollution rules around the world. Also, because it uses non-edible oil and helps burn fuel better, it's a smart and eco-friendly option for the future. Stakeholders can utilize this information to enhance engine performance and combustion behavior. However, the use of nanoparticles in fuels, particularly metal oxide nanoparticles, presents new challenges concerning particulate matter emissions. Additional research is needed to understand and address the impact of these nanoparticles on emissions and develop appropriate measures for emission control.

ABBREVIATIONS

ANOVA	Analysis of variance
DOE	Design of the experiment
BTE	Brake thermal efficiency
BSFC	Brake specific fuel consumption (Kg/Kw Hr)
TFC	Total fuel consumption (Kg/Hr)
TiO_2	Titanium Dioxide
CO	Carbon monoxide
CO_2	Carbon dioxide
HC	Hydrocarbons

NO_X	Nitrogen oxides
SOx	Sulfur oxide
RSM	Response Surface Modeling
L	Load on Engine
B	Rice Bran Bio-Diesel blend
N	Nanoparticle, α- significance factor
CI	Compression Ignition

AUTHORSHIP CONTRIBUTIONS

Authors equally contributed to this work.

DATA AVAILABILITY STATEMENT

The authors confirm that the data that supports the findings of this study are available within the article. Raw data that support the finding of this study are available from the corresponding author, upon reasonable request.

CONFLICT OF INTEREST

The author declared no potential conflicts of interest with respect to the research, authorship, and/or publication of this article.

ETHICS

There are no ethical issues with the publication of this manuscript.

STATEMENT ON THE USE OF ARTIFICIAL INTELLIGENCE

Artificial intelligence was not used in the preparation of the article.

REFERENCES

[1] Singh Pali H, Kumar M, Nguyen NV, Singh Y, Deepanraj B, Quy P, et al. Enhancement of combustion characteristics of waste cooking oil biodiesel using TiO2 nanofluid blends through RSM. Fuel 2023;331:125681−125681. [Crossref]

[2] Balajii M, Niju S. Esterification optimization of underutilized Ceiba pentandra oil using response surface methodology. Biofuels 2021;12:495−502. [Crossref]

[3] Rajak R, Chattopadhyay A. Short and Long Term Exposure to Ambient Air Pollution and Impact on Health in India: A Systematic Review. Int J Environ Health Res 2020;30:593−617. [Crossref]

[4] Walsh MP. Mobile source related air pollution: Effects on health and the environment. Encycl Environ Heal 2019;436−442. [Crossref]

[5] International Energy Agency. World Energy Outlook 2021. Available at: https://www.iea.org/reports/world-energy-outlook-2021 Accessed on Sep 5, 2025

[6] US Energy Information Administration (EIA). International Energy Outlook 2017 Overview. Available at: https://www.eia.gov/outlooks/ieo/pdf/0484(2017).pdf. Accessed on Sep 5, 2025

[7] Sustainable T, Project M. Mobility 2030. World Bussiness Counc Sustain Dev 2014.

[8] ROOT MH. International Energy Agency 2012. Available at https://www.iea.org/reports/world-energy-outlook-2012

[9] Dye C, Reeder JC, Terry RF. Research for universal health coverage. Sci Transl Med. 2013;5:199. [Crossref]

[10] S. L. C. Richard PK, Allan, Arias PA, Berger S, Canadell JG, Cassou C , Chen D, Cherchi A. Climate Change 2021. Available at: https://www.ipcc.ch/report/ar6/wg1/. Accessed on Sep 5, 2025

[11] Raheman H, Phadatare AG. Performance of compression ignition engine with mahua (Madhuca indica) biodiesel. Fuel 2007;86:2568−2573. [Crossref]

[12] Makepa DC, Chihobo CH, Musademba D. Advances in sustainable biofuel production from fast pyrolysis of lignocellulosic biomass. Biofuels. 2023;14:529−550. [Crossref]

[13] Chandrasekaran V, Arthanarisamy M, Nachiappan P, Dhanakotti S, Moorthy B. The role of nano additives for biodiesel and diesel blended transportation fuels. Transp Res Part D Transp Environ. 2016;46:145−156. [Crossref]

[14] Sundar SP, P Vijayabalan, Hemalatha D, Ramani B, Chamkha JA, Sathyamurthy R, et al. Feasibility study of neat plastic oil with TiO_2 nanoadditive as an alternative fuel in internal combustion engine. J Therm Anal Calorim 2022;147:2567−2578. [Crossref]

[15] Fasogbon SK, Oyedepo SO. Nano-additive blends examination of performance and emission profile of CI engines fuelled with waste cooking oil based-biodiesel. J Therm Eng. 2025;11:1−15. [Crossref]

[16] Khankal D, Hole S, Gadekar H, Jagtap A, Pandhare A. Comparative analysis of performance and emission from single cylinder diesel engine fuelled with mango kernel biodiesel. J Therm Eng 2024;10:1632−1646. [Crossref]

[17] Yamini K, Kishore PS, Dhana Raju V. Effect of diethyl ether and isobutanol as fuel additives on the diesel engine attributes fueled with subabul seed biodiesel. J Therm Eng 2025;11:215−225. [Crossref]

[18] Sharma P, Le MP, Chhillar A, Said Z, Deepanraj B, Cao DN, et al. Using response surface methodology approach for optimizing performance and emission parameters of diesel engine powered with ternary blend of Solketal-biodiesel-diesel. Sustain Energy Technol Assessments 2022;52. [Crossref]

[19] I Veza, Karaoglan AD, Ileri E, Afzal A, Hoang AT, Tamaldin N, et al. Multi-objective optimization of diesel engine performance and emission using grasshopper optimization algorithm. Fuel 2022;323. [Crossref]

[20] Gbadeyan OJ, Muthivhi J, Linganiso LZ, Mpongwana N, Dziike F, Deenadayalu N. Recent improvements to ensure sustainability of biodiesel production. Biofuels 2024;15:1063–1077. [Crossref]
[21] Rajan K, Prabhahar M, Senthilkumar KR. Experimental studies on the performance, emission and combustion characteristics of a biodiesel-fuelled (Pongamia methyl ester) diesel engine with diethyl ether as an oxygenated fuel additive. Int J Ambient Energy 2016;37:439–445. [Crossref]
[22] Kumar S, Dinesha P, Bran I. Influence of nanoparticles on the performance and emission characteristics of a biodiesel fuelled engine: An experimental analysis. Energy 2017;140:98–105. [Crossref]
[23] ASTM D6751-15c. Standard Specification for Biodiesel Fuel Blend Stock (B100) for Middle Distillate Fuels. ASTM Int 2010;i:1–11.
[24] Prasad A, Sivanraju R, Teklemariam A, Tafesse D, Tufa M, Bejaxhin BH. Influence of nano additives on performance and emissions characteristics of a diesel engine fueled with watermelon methyl ester. J Therm Eng 2023;9:395–400. [Crossref]
[25] Machado Corrêa S, Arbilla G. Carbonyl emissions in diesel and biodiesel exhaust. Atmos Environ 2008;42:769–775. [Crossref]
[26] Raheman H, Phadatare AG. Diesel engine emissions and performance from blends of karanja methyl ester and diesel. Biomass Bioenergy 2004;27:393–397. [Crossref]
[27] Venkata Subbaiah G, Raja Gopal K. An experimental investigation on the performance and emission characteristics of a diesel engine fuelled with rice bran biodiesel and ethanol blends. Int J Green Energy 2011;8:197–208. [Crossref]
[28] Alam A, Kalam MA, Habibullah M, Hossain MM, Masjuki HH, Rashedul HK, et al. Impact of edible and non-edible biodiesel fuel properties and engine operation condition on the performance and emission characteristics of unmodified DI diesel engine. Biofuels 2016;7:219–232. [Crossref]
[29] Çalhan R, Kaskun Ergani S. The impacts of nano fuels containing Fe-Ni-TiO_2/activated carbon nanoparticles on diesel engine performance and emission characteristics. Biofuels 2023;14:661–671. [Crossref]
[30] Kumar S, Dinesha P, Bran I. Experimental investigation of the effects of nanoparticles as an additive in diesel and biodiesel fuelled engines: a review. Biofuels 2019;10:615–622. [Crossref]
[31] Jaikumar S, Srinivas V, Rajasekhar M. Influence of dispersant added nanoparticle additives with diesel-biodiesel blend on direct injection compression ignition engine: Combustion, engine performance, and exhaust emissions approach. Energy 2021;224:120197. [Crossref]
[32] Mahalingam S, Ganesan S. Effect of nano-fuel additive on performance and emission characteristics of the diesel engine using biodiesel blends with diesel fuel. Int J Ambient Energy 2020;41:316–321. [Crossref]
[33] Soudagar MEM, Nik-Ghazali NN, Abul Kalam M, Badruddin IA, Banapurmath NR, Akram N. The effect of nano-additives in diesel-biodiesel fuel blends: A comprehensive review on stability, engine performance and emission characteristics. Energy Convers Manag 2018;178:146–177. [Crossref]
[34] Yusof SNA, Sidik NAC, Asako Y, Japar WMAA, Mohamed SB, az Muhammad NM. A comprehensive review of the influences of nanoparticles as a fuel additive in an internal combustion engine (ICE). Nanotechnol Rev 2021;9:1326–1349. [Crossref]
[35] Giwa SO, Aasa SA, Shote AS, Sharifpur M. Nanoparticles-suspended biodiesel and its blends in compression ignition engines: a bibliometric analysis of research trend and future outlook. Biofuels 2023;14:673–686. [Crossref]
[36] Dehhaghi M, Kazemi Shariat Panahi H, Aghbashlo M, Lam SS, Tabatabaei M. The effects of nanoadditives on the performance and emission characteristics of spark-ignition gasoline engines: A critical review with a focus on health impacts. Energy 2021;225:120259. [Crossref]
[37] Hosseini SH, Taghizadeh-Alisaraei A, Ghobadian B, Abbaszadeh-Mayvan A. Effect of added alumina as nano-catalyst to diesel-biodiesel blends on performance and emission characteristics of CI engine. Energy 2017;124:543–552. [Crossref]
[38] Manzoor Q, et al. Toxicity spectrum and detrimental effects of titanium dioxide nanoparticles as an emerging pollutant: A review. Desalin Water Treat 2024;317:100025. [Crossref]
[39] Jain A, Ambekar A, Thajudeen T. Effect of Titania Nano-additives on Fine and Ultrafine Carbonaceous Emissions during Flame Combustion of Diesel. Aerosol Air Qual Res 2024;24. [Crossref]
[40] Yamin J, Hdaib II, Eh Sheet EA, Abu Mushref AJ. RSM analysis of heat balance of direct injection 4-stroke diesel engine using biodiesel fuel. Biofuels 2021;12:777–787. [Crossref]
[41] Chinmaya M, Anuj P, Singh TV, Naveen K. Combustion, Emission and Performance Characteristics of a Light Duty Diesel Engine Fuelled with Methanol Diesel Blends. Int J Mech Mechatronics Eng 2013;7:40–50.
[42] Jayaraman J, Alagu K, Venu H, Appavu P, Joy N, Jayaram P, Mariadhas A. Enzymatic production of rice bran biodiesel and testing of its diesel blends in a four-stroke CI engine. Energy Sources Part A Recover Util Environ Eff 2023;45:5340–5351. [Crossref]
[43] Hotti SR, Hebbal OD. Biodiesel production and fuel properties from non-edible champaca (Michelia champaca) seed oil for use in diesel engine. J Therm Eng 2015;1:330–336. [Crossref]

[44] Kayode B, Hart A. An overview of transesterification methods for producing biodiesel from waste vegetable oils. Biofuels 2019;10:419–437. [Crossref]

[45] Bohlouli A, Mahdavian L. Catalysts used in biodiesel production: a review. Biofuels. 2021;12:885–898. [Crossref]

[46] Ghanati SG, Doğan B, Yeşilyurt MK. The effects of the usage of silicon dioxide (SiO_2) and titanium dioxide (TiO_2) as nano-sized fuel additives on the engine characteristics in diesel engines: a review. Biofuels 2024;15:229–243. [Crossref]

[47] Drews A. Standard Test Method for Kinematic Viscosity of Transparent and Opaque Liquids (the Calculation of Dynamic Viscosity). In Manual on Hydrocarbon Analysis.6th ed. Pennsylvania, USA: ASTM Manuals; 2008. p. 126–128. [Crossref]

[48] Tomar M, Kumar N. Influence of nanoadditives on the performance and emission characteristics of a CI engine fuelled with diesel, biodiesel, and blends–a review. Energy Sources Part A Recover Util Environ Eff 2020;42:2944–2961. [Crossref]

[49] Drews A. Standard Practice for Density, Relative Density (Specific Gravity), or API Gravity of Crude Petroleum and Liquid Petroleum Products by Hydrometer Method. In Manual on Hydrocarbon Analysis.6th ed. Pennsylvania, USA: ASTM Manuals 2008. p. 252–255. [Crossref]